Biophysical Chemistry 135 (2008) 102–109

Contents lists available at ScienceDirect

Biophysical Chemistry

journal homepage: http://www.elsevier.com/locate/biophyschem

Tricationic pyridium porphyrins appending different peripheral substituents: Experimental and DFT studies on their interactions with DNA

Ping Zhao [a], Lian-Cai Xu [a], Jin-Wang Huang [a,b,*], Kang-Cheng Zheng [a], Bo Fu [a], Han-Cheng Yu [a], Liang-Nian Ji [a,b,c]

[a] MOE Laboratory of Bioinorganic and Synthetic Chemistry, School of Chemistry and Chemical Engineering, Sun Yat-Sen University, Guangzhou 510275, PR China
[b] State Key Laboratory of Optoelectronic Material and Technologies, Sun Yat-Sen University, Guangzhou 510275, PR China
[c] The Key Laboratory of Gene Engineering of Ministry of Education, Sun Yat-Sen University, Guangzhou 510275, PR China

ARTICLE INFO

Article history:
Received 21 January 2008
Received in revised form 29 March 2008
Accepted 30 March 2008
Available online 7 April 2008

Keywords:
Cationic porphyrin
DNA-binding
Photocleavage
DFT

ABSTRACT

Four tricationic pyridium porphyrins appending hydroxyphenyl, methoxyphenyl, propionoxyphenyl or carboxyphenyl group at *meso*-20-position of porphyrin core have been synthesized and their abilities to bind and cleave DNA have been investigated. Using a combination of absorption, fluorescence, circular dichroism (CD) spectra, thermal DNA denaturation as well as viscosity measurements, their binding modes and intrinsic binding constants (K_b) to calf DNA (CT DNA) were comparatively studied and also compared with those of 5,10,15,20-tetrakis(1-methylpyridinium-4-yl)porphyrin (TMPyP). The results suggest that the K_b values of these porphyrins are greatly influenced by the number of positive charges and steric hindrance. Theoretical calculations applying the density functional theory (DFT) have been carried out and explain their DNA-binding properties reasonably. The efficiency of DNA photocleavage by these porphyrins shows high dependence on the values of K_b.

© 2008 Elsevier B.V. All rights reserved.

1. Introduction

TMPyP (see structure in Fig. 1, compound **1**) is a water-soluble cationic porphyrin and has been extensively studied in recent years, especially in relation to its unique physicochemical properties which lead to its tight interaction with nucleic acids and widespread therapeutic application [1–13]. Pasternack and Sobell have constructed a stable molecular models for the B-DNA–TMPyP complex in which the porphyrin core intercalates into DNA base-pairs and the positively charged, *meso*-substituents interact with the negatively charged phosphate groups of the DNA backbone [14]. Although TMPyP is a good model for DNA-binding research, its practical application in clinic is often restricted by its stable methylpyridinium substituents. Thus, pyridium porphyrins appending active substituents attract a great deal of interests since they are expected to have not only similar DNA-binding behaviors to TMPyP but also wider practical application through coupling with other bioactive molecules. Some researches have been developed on the interactions between TMPyP-like cationic porphyrins and DNA [15–20]. We have also recently investigated the DNA-binding and cleavage behaviors of a tricationic pyridium porphyrin bearing an anthraquinone chromophore [21]. The experimental results of these studies show that the introduction of active substituent groups may greatly change the physicochemical characters of these pyridium porphyrins and thus leads to quite different DNA-binding and cleaving properties.

In addition to the experimental efforts, various theoretical researchers have been trying to correlate some theoretical predictions to the experimental findings on the interaction between drugs and DNA. Kurita and Kobayashi [22] reported the density functional MO (molecular orbital) calculations for stacked DNA base-pair model with backbones, and their calculated results show that the energies of the HOMO (the highest occupied molecular orbital) and occupied MOs near HOMO are rather high and their components are mainly distributed on the base-pairs of DNA. Therefore, Kurita's results offered a theoretical foundation for the base-pairs of DNA being good electron donors in the interactions between drugs and DNA. We have also reported some DFT results on the electronic structures and related properties of some Ru(II) polypyridyl complexes [23–26], and hereby successfully discussed their DNA-binding trends and related properties. These theoretical efforts at the level of molecular electronic structures of the complexes and DNA are very significant in guiding experimental works. However, up to now, there have been few theoretical reports focusing on explanation of the interactions between TMPyP-like porphyrins and DNA [21].

Herein, we synthesized four tricationic pyridium porphyrins (see structures in Fig. 1, compounds **2**, **3**, **4**, **5**) appending hydroxyphenyl,

* Corresponding author. MOE Laboratory of Bioinorganic and Synthetic Chemistry, School of Chemistry and Chemical Engineering, Sun Yat-Sen University, Guangzhou 510275, PR China. Tel.: +86 20 84113317; fax: +86 20 84112245.
E-mail address: ceshjw@163.com (J.-W. Huang).

0301-4622/$ – see front matter © 2008 Elsevier B.V. All rights reserved.
doi:10.1016/j.bpc.2008.03.013

methoxyphenyl, propionoxyphenyl or carboxyphenyl group, respectively, and studied their binding properties with CT DNA. Meanwhile, the theoretical calculations applying DFT were also carried out to explain their DNA-binding behaviors. Finally, the photocleavage of pBR322 plasmid DNA by these porphyrins were investigated. For the purpose of comparison, the DNA-binding and photocleavage behaviors of TMPyP were also investigated under identical experimental conditions.

2. Experimental

2.1. Synthesis of porphyrins

The classical Adler–Longo method [27] was used to synthesize the title porphyrins. A mixture of propionic acid, acetic anhydride and corresponding aldehyde was heated at 130 °C with stirring. 4-pyridinecarboxaldehyde and pyrrole were then added separately from dropping funnels to the refluxing mixture. The resulting mixture was refluxed for 1.5 h. The solvent was subsequently evaporated under reduced pressure. The residue was then purified by column chromatography. Methylation by an excess amount of methyl iodide afforded target compounds **1–5**.

The spectroscopic results obtained from TMPyP **(1)**: ^{1}H NMR (300 MHz, DMSO): chemical shift δ: 9.45(d, *J*=6.0 Hz, 6H, 2, 6-pyridinium), 8.99–9.01(s, 8H, β-pyrrole), 8.27(d, *J*=7.8 Hz, 6H, 3,5-pyridinium), 4.69(s, 9H, N$^+$–Me), −3.01(s, 2H, NH pyrrole). ES-MS [EtOH, *m*/*z*]: 678 ([M]$^+$), 169 ([M]$^{4+}$). UV–Vis (10 μM in Tris buffer), λ_{max}(nm) (log ε): 423(4.63), 517(3.39), 562(3.48), 585(3.00), 643(2.99).

The spectroscopic results obtained from 5,10,15-tris(1-methylpyridinium-4-yl)-20-(4-hydroxyphenyl)porphyrin **(2)**: ^{1}H NMR (300 MHz, DMSO): chemical shift δ: 9.448(d, *J*=5.94 Hz, 6H, 2, 6-pyridinium), 9.12(s, 4H, β-pyrrole), 9.05(s, 4H, β-pyrrole), 8.978(d, *J*=5.51 Hz, 6H, 3, 5-pyridinium), 8.00(d, *J*=8.13 Hz, 2H, 2, 6-phenyl), 7.255(d, *J*=8.06 Hz, 2H, 3, 5-phenyl), 4.711(s, 9H, N$^+$–Me), 3.00(s, 1H, OH), −2.957(s, 2H, NH pyrrole). ES-MS [EtOH, *m*/*z*]: 678 ([M]$^+$), 339 ([M]$^{2+}$), 226 ([M]$^{3+}$). UV–Vis (10 μM in Tris buffer), λ_{max}(nm) (log ε): 425(4.9), 523(3.72), 562(3.48), 583(3.48), 641(3.04).

The spectroscopic results obtained from 5,10,15-tris(1-methylpyridinium-4-yl)-20-(4-methoxyphenyl)porphyrin **(3)**: ^{1}H NMR (300 MHz, DMSO): chemical shift δ: 9.46 (d, *J*=5.96 Hz, 6H, 2, 6-pyridinium), 9.15 (s, 4H, β-pyrrole), 9.05 (s, 4H, β-pyrrole), 8.99 (d, *J*=5.49 Hz, 6H, 3, 5-pyridinium), 8.14 (d, 2H, 2,6-phenyl), 7.44 (d, *J*=8.06 Hz, 2H, 3,5-phenyl), 4.72 (s, 9H, N$^+$–Me), 4.00(s, 3H, CH_3). ES-MS [EtOH, *m*/*z*]: 692 ([M]$^+$), 346 ([M]$^{2+}$), 231 ([M]$^{3+}$). UV–Vis (10 μM in Tris buffer), λ_{max} (nm) (log ε): 425(5.09), 522(3.94), 560(3.70), 581(3.66), 644(3.28).

The spectroscopic results obtained from 5,10,15-tris(1-methylpyridinium-4-yl)-20-(4-propionoxyphenyl)porphyrin **(4)**: ^{1}H NMR (300 MHz, DMSO): chemical shift δ: 9.46(d, *J*=5.81 Hz, 6H, 2, 6-pyridinium), 9.16(s, 4H, β-pyrrole), 9.07(s, 4H, β-pyrrole), 9.00(d, 6H, 3, 5-pyridinium), 8.26(d, *J*=5.53 Hz, 2H, 2,6-phenyl), 7.65(d, *J*=8.45 Hz, 2H, 3,5-phenyl), 4.72 (s, 9H, N$^+$–Me), 1.30 (s, 3H, CH_3). ES-MS [EtOH, *m*/*z*]: 735 ([M]$^+$), 367 ([M]$^{2+}$), 245([M]$^{3+}$). UV–Vis (10 μM in Tris buffer), λ_{max} (nm) (log ε) 422(5.07), 520(3.84), 562(3.60), 583(3.56), 642(3.19).

The spectroscopic results obtained from 5,10,15-tris(1-methylpyridinium-4-yl)-20-(4-carboxyphenyl)porphyrin **(5)**: ^{1}H NMR (300 MHz, DMSO): chemical shift δ: 13.00(s, 1H, carboxyl), 9.44(d, *J*=5.94 Hz, 6H, 2,6-pyridinium), 8.99–9.10(s, 8H, β-pyrrole), 8.22(d, *J*=5.64 Hz, 6H, 3,5-pyridinium), 8.12(d, *J*=7.8 Hz, 2H, 2,6-phenyl), 8.00 (d, *J*=8.07 Hz, 2H, 3,5-phenyl), 4.70(s, 9H, N+–Me), −2.98 (s, 2H, NH pyrrole). ES-MS [EtOH, *m*/*z*]: 706 ([M]$^+$), 353 ([M]$^{2+}$), 235 ([M]$^{3+}$). UV–Vis (10 μM in Tris buffer), λ_{max}(nm) (log ε) 422(4.79), 521(3.52), 553(3.34), 585(3.21), 641(2.38).

2.2. Characterization measurements

^{1}H NMR spectra were recorded on a Varian-300 spectrometer. All chemical shifts are given relative to tetramethylsilane (TMS). Electrospray mass spectra (ES-MS) were recorded on a LCQ system (Finnigan MAT, USA). The spray voltage, tube lens offset, capillary voltage and capillary temperature were set at 4.50 kV, 30.00 V, 23.00 V and 200 °C, respectively, and the quoted *m*/*z* values are for the major peaks in the isotope distribution. UV–Vis spectra were recorded on a Perkin-Elmer-Lambda-850 spectrophotometer. Flash chromatography was performed using silica gel (200–300 mesh). Unless otherwise stated, reagents were commercially available and of analytical grade.

2.3. Measurements of porphyrin–CT DNA interactions

Buffer A (5 mM Tris–HCl, 50 mM NaCl, pH=7.2, Tris=Tris (hydroxymethyl)aminomethane) solution was used in all the experiments except for the thermal denaturation studies in which buffer B (1.5 mM Na_2HPO_4, 0.5 mM NaH_2PO_4, 0.25 mM Na_2H_2EDTA (H_4EDTA=*N*,*N*′-ethane-1,2-diylbis[*N*-(carboxymethyl)glycine]), pH 7.0) was used. CT DNA was obtained from the Sigma Company. A solution of CT DNA in the buffer A gave a ratio of UV absorbance at 260 and 280 nm of 1.85:1, indicating that the DNA was sufficiently free of protein. The DNA concentration per nucleotide was determined by absorption spectroscopy using the molar absorption coefficient (6600 M^{-1} cm^{-1}) at 260 nm [28].

UV–Vis spectra were recorded on a Perkin-Elmer-Lambda-850 spectrophotometer. Emission spectra were recorded on a Perkin-Elmer L55 spectrofluorophotometer at room temperature. CD Spectra were recorded on a JASCO-J810 spectrometer.

Thermal denaturation studies were carried out with a Perkin-Elmer-Lambda-850 spectrophotometer equipped with a Peltier temperature-controlling programmer (±0.1 °C). The melting curves were obtained by measuring the absorbance at 260 nm for solutions of CT DNA (100 μM) in the absence and presence of the porphyrin compound (10 μM) as a function of the temperature. The temperature was scanned from 30 to 90 °C at a speed of 1 °C min^{-1}. The melting temperature (T_m) was taken as the mid-point of the hyperchromic transition.

For the gel electrophoresis experiment, pBR322 supercoiled plasmid DNA (0.1 μg) was treated with the porphyrin compound in buffer C (50 mM Tris–HCl, 18 mM NaCl, pH=7.2), and the solution was then irradiated at room temperature with a high pressure mercury lamp/monochromator assembly. The samples were analyzed by electrophoresis for 1 h at 120 V in Tris-acetate buffer containing 1% agarose gel. The gel was stained with 1 μg ml^{-1} ethidium bromide and photographed under UV light.

2.4. Theoretical detail

The structural sketches of all studied porphyrins **1–5** with no symmetry were shown in Fig. 1. The full geometry optimization and

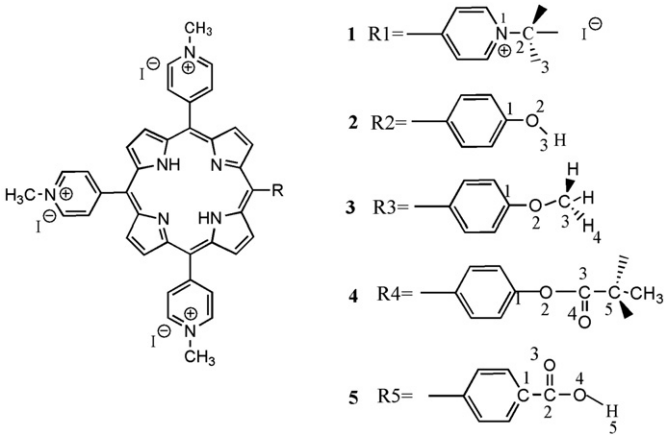

Fig. 1. The molecular structures of porphyrins **1**–**5**.

Table 1
Physical data of porphyrins **1**–**5** binding with CT DNA

Porphyrin	UV–Vis titration		Fluorescence titration	CD spectra (nm)		ΔT_m (°C)	K_b
	Δλ (nm)	% H	Increase (%)	+	−		
1	12	48.3	55		445	12.2	2.1×10^6
2	10	47.5	52		443	9.1	4.9×10^5
3	8	46.9	48	425	448	4.7	6.81×10^4
4	7	36.7	40	427	446	4.0	6.43×10^4
5	5	30.6	33	424	447	1.5	5.17×10^4

further frequency analysis were carried out with the DFT-B3LYP method and 6-31G basis set, and single point calculation was further performed based on the level of B3LYP/6-31G*. In order to vividly depict the detail of the frontier molecular orbital, the stereographs of some related frontier molecular orbits of these complexes were drawn with the Molden v 4.2 program based on the calculated results. All calculations were performed with the G03 (d01) program-package [29].

3. Results and discussion

3.1. Binding studies

3.1.1. Absorption titrations

One of the most common techniques in DNA-binding studies of porphyrins is electronic absorption spectroscopy. The magnitude of spectral perturbation is an evidence for DNA-binding [2,4]. As is well known, intercalation of porphyrin into DNA base-pairs is characterized by a red shift (>10 nm) and intensity decrease (up to 40%) in the Soret band of UV–Vis spectra; groove binding mode shows no (or minor) change in UV–Vis spectra while outside binding mode exhibits moderate red shift and intensity decrease in the Soret band of porphyrins [2,3,6,9,20]. All physical data about the change of porphyrins' absorption spectra in the presence of increasing amounts of CT DNA are collected in Table 1. A representative example (of porphyrin **5**) is shown in Fig. 2 and analogous spectra were obtained in the case of other four porphyrins. With increasing CT DNA concentration, different extents of red shift and intensity decrease are found in the Soret bands for the five compounds, indicating different DNA-binding modes of them. The large red shift and intensity decrease of **1** and **2** (12 nm and 48.3%, 10 nm and 47.5%, respectively) indicates that the two porphyrins may intercalate into DNA and the moderate changes in the absorbance spectra of **3**, **4**, **5** suggest that these three may employ outside binding mode.

In order to compare quantitatively the affinities of the compounds bound to CT DNA, the intrinsic binding constants K_b were measured by monitoring the changes of absorbance in the Soret band with increasing concentration of CT DNA using the following equation [14].

$$[\mathrm{DNA}]/(\varepsilon_a-\varepsilon_f)=[\mathrm{DNA}]/(\varepsilon_b-\varepsilon_f)+1/\{K(\varepsilon_b-\varepsilon_f)\}$$

where [DNA] is the concentration of DNA in base-pairs, ε_a, ε_f and ε_b correspond to the apparent absorption coefficient Aobsd/[Por] ([Por], the concentration of porphyrin), the extinction coefficient for the free porphyrin complex and the extinction coefficient for the porphyrin complex in the fully bound form, respectively. From the plot of [DNA]/($\varepsilon_a-\varepsilon_f$) versus [DNA], K_b of the porphyrin compounds were calculated and the results were listed in Table 1, too.

From Table 1, we can find that the values of K_b are sensitive to the precise structure of porphyrins, following an order of **1**>>**2**>**3**>**4**>**5**. The much larger K_b of the tetracationic porphyrin suggests that the number of positive charges is the main factor to affect the binding affinity. This somewhat expected result may result from the stronger electrostatic effect between **1** and the negative DNA backbone than the tricationic porphyrins. Moreover, porphyrin **2** shows relatively larger binding ability comparing with other three tricationic analogs, indicating that the steric hindrance may also be an important factor since **2** has a relatively smaller steric hindrance than **3**, **4**, **5**. Porphyrin **5** shows a relatively low binding constant ($K_b=5.17\times10^4$),

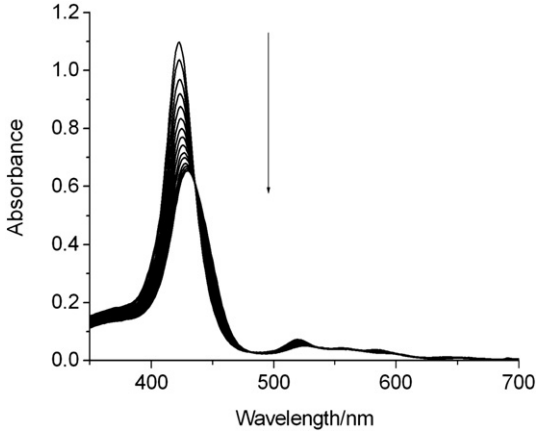

Fig. 2. Absorption spectrum of **5** in buffer A at 25 °C in the presence of increasing amounts of CT DNA. [Por]=10 μM, [DNA]=0–26.4 μM from top to bottom. Arrow indicates the change in absorbance upon increasing the DNA concentration.

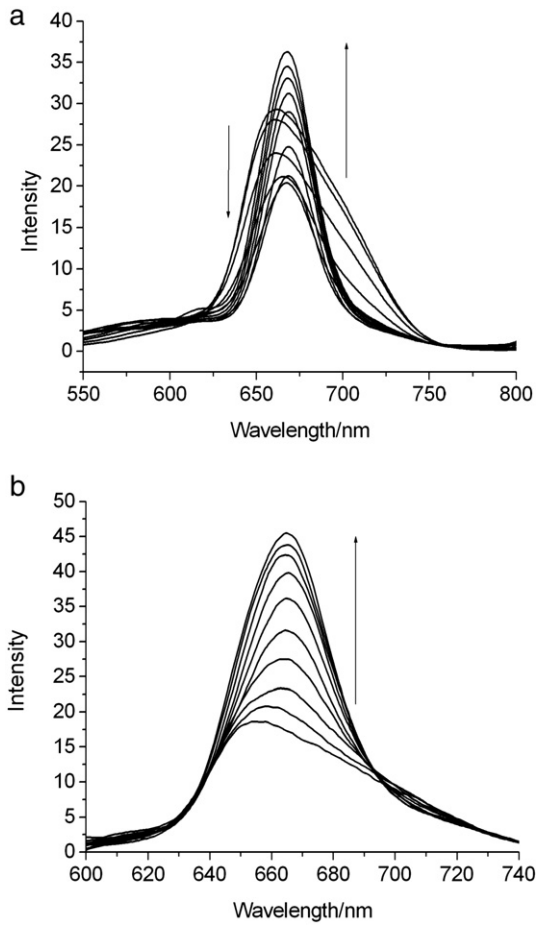

Fig. 3. Emission spectra of porphyrins **2** (a) and **3** (b) in buffer A at 25 °C in the presence of CT DNA. [Por]=10 μM. The arrows show the intensity changes upon increasing DNA concentration.

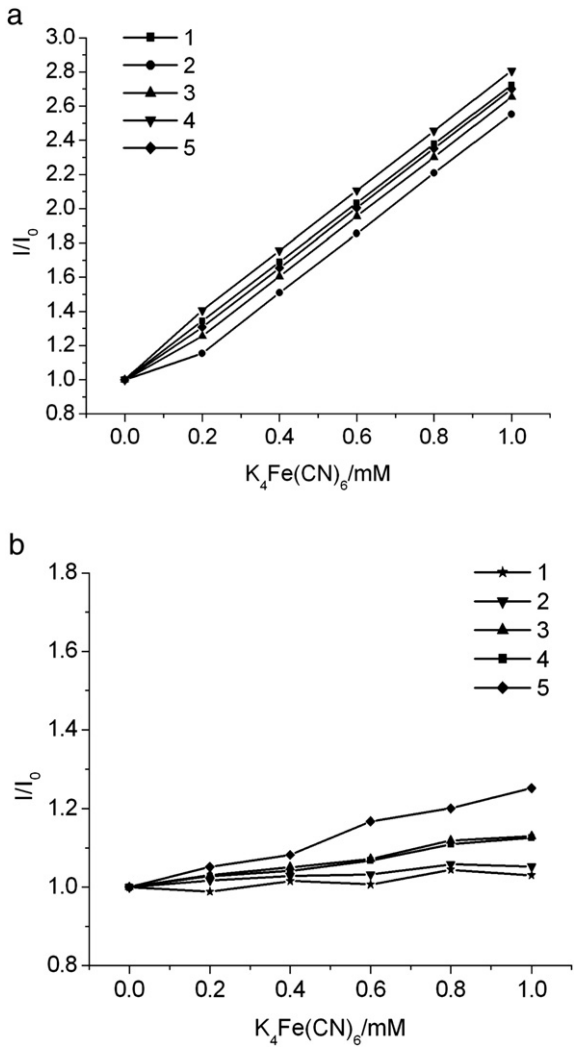

Fig. 4. Steady-state quenching of emission for porphyrins alone (a) and in the presence of 1:4 porphyrin to DNA in buffer A by potassium ferrocyanide (b). I and I_0 are the luminescence intensities in the absence and presence of $[Fe(CN)_6]^{4-}$, respectively.

which may due to its electronegative carboxyphenyl group ([20] and theoretical calculations below).

3.1.2. Fluorescence titration

Fluorescence decay experiments in the presence of CT DNA were performed. With increasing of the DNA concentration, large increases in intensities of fluorescence emission (see Table 1) are depicted for all porphyrins, which imply that all compounds can interact with DNA and be protected by DNA efficiently, since the hydrophobic environment inside the DNA helix reduces the accessibility of solvent water molecules to the compound.

Fluorescence emission spectra of porphyrins **2** and **3** are selected to show the spectral change with increasing DNA (Fig. 3). It is notable that **2** exhibits remarkable decrease in intensity of fluorescence emission at the initial stage of DNA titration (Fig. 3a). It can be ascribed to self-stacking of the porphyrin molecules along the DNA surface [30], and is thought to be a criterion for intercalation [31]. Similar phenomenon is also previously observed for porphyrin **1** [32–34]. However, there are no obvious decreases that appear in the fluorescence intensity of **3** at low concentrations of DNA (Fig. 3b), and analogous spectra were gained in the case of **4** and **5**. These results further suggest that intercalation could not occur in the binding of porphyrins **3**, **4** and **5** to DNA [31].

Steady-state emission quenching experiments using potassium ferrocyanide ($K_4Fe(CN)_6$) as a quencher were also used to observe the binding of porphyrins to CT DNA. As illustrated in Fig. 4a, the fluorescence emission intensities of porphyrins **1–5** in the absence of DNA are efficiently quenched by $[Fe(CN)_6]^{4-}$. However, in the presence of DNA, the slopes of the plot are remarkably decreased (Fig. 4b). This may be explained by the fact that the bond cations of the compounds are protected from the anionic water-bound quencher by the array of negative charges along the DNA phosphate backbone. The curvature reflects different degrees of protection or relative accessibility of bound cations [35]. Fig. 4 clearly shows that the curvature extent order of the five porphyrins is **1**>**2**>**3**>**4**>**5** in the present of DNA. Accordingly, the DNA-binding affinity follows an order that **1**>**2**>**3**>**4**>**5**. Such a trend is consistent with the trend of DNA-binding affinities which was observed in absorption titrations.

3.1.3. Circular dichroism (CD) studies

The circular dichroism (CD) spectrum experiment may be one of the most direct means in examining the binding modes of the porphyrin compounds to DNA. The sign of the induced CD spectrum of DNA in the Soret region can be used as a sensitive signature for the binding modes of porphyrins to DNA: a positively induced CD band is indicative of external (minor groove) binding, a negatively induced CD band is produced upon intercalation and a conservative bisignal induced CD band is the characteristic of outside binding [14,20,36–38].

Fig. 5 and Table 1 give the results of CD studies which were also carried out to investigate the binding modes of the cationic porphyrins. Porphyrins do not yield any CD signal in the absence of DNA (data not shown). As shown in Fig. 5, CD spectra were induced for the porphyrins in the presence of DNA, due to the interaction between the transition moments of the achiral porphyrin and chirally arranged DNA base transitions. Porphyrins **1** and **2** show strong negative peaks centered at *ca.* 445 nm upon binding to CT DNA, suggesting that they are excellent DNA intercalators. As to porphyrins **3**, **4** and **5**, positive CD spectra in the range of 410–430 nm and negative CD spectra in the range of 430–460 nm were observed, which is consistent with outside binding mode. The result of CD experiment unambiguously proves the binding modes we proposed in the absorption and fluorescence experiments.

3.1.4. Thermal denaturation studies

The melting temperature (T_m) of DNA is sensitive to its double helix stability and the binding of compounds to DNA alters the T_m depending on the strength of interactions [2]. Therefore, it can be used as an indicator of binding properties of porphyrins to DNA and their

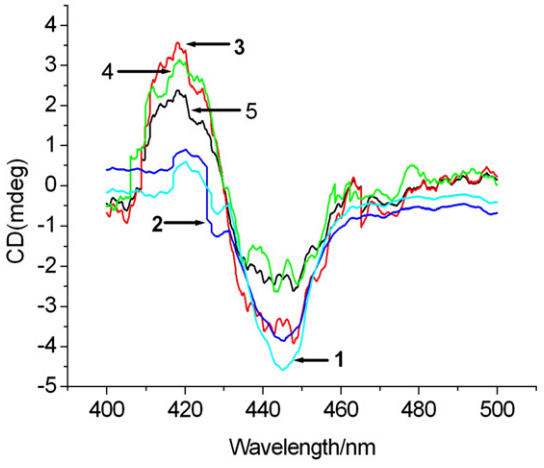

Fig. 5. Induced CD spectra of porphyrins in the presence of CT DNA in buffer A. [Por] = 6.4 μM, [DNA] = 48 μM.

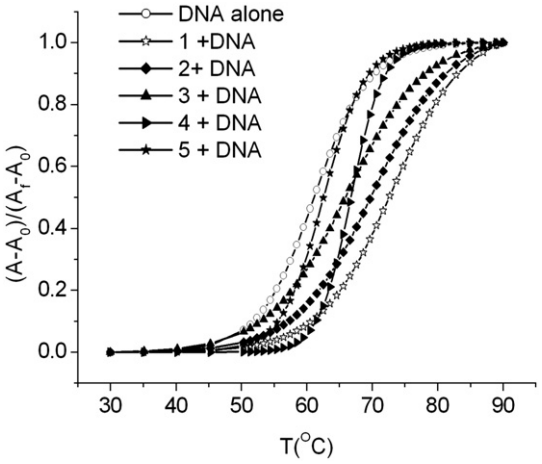

Fig. 6. Melting curves of CT DNA at 260 nm in the absence and the presence of porphyrins, in buffer B. [Por] = 10 μM, [DNA] = 100 μM.

binding strength. T_m will considerably increase when intercalation binding mode occurs [14,39].

The melting curves of CT DNA in the absence and presence of porphyrins are presented in Fig. 6. The T_m of CT DNA is (61.1 ± 0.2) °C in the absence of the compounds. When mixed with the compounds at a concentration ratio [Por]/[DNA] of 1:10, the observed melting temperatures of CT DNA increase to different degrees. The differences, designed as ΔT_m, are collected in Table 1. Here, $\Delta T_m = T_m - T_m^0$, T_m and T_m^0 refer to the melting temperature of DNA in the presence and absence of compounds, respectively.

The large increases of T_m in the presence of **1** and **2** (ΔT_m = 12.0 °C and 9.1 °C, respectively) indicate that the compound molecules interact with DNA in a typical intercalative mode and have strong DNA-binding affinities. The small increases of T_m in the presence of porphyrins **3** and **4** (ΔT_m = 4.7 °C, 4.0 °C, relatively) reveal that a few molecules of these porphyrins also intercalate into the DNA duplex at this [Por]/[DNA] ratio. However, the negligible increase of T_m in the presence of porphyrin **5** (ΔT_m = 1.5 °C) gives us the information that this compound doesn't intercalate into DNA and has a relatively weak DNA-binding affinity. These results are in good agreement with the experiments above.

3.1.5. Viscosity measurement

In the absence of X-ray structural data, viscosity measurement is regarded as the least ambiguous and the most critical test of a DNA-binding model in solution and provides strong arguments for intercalative DNA-binding mode. Intercalative mode is expected to lengthen the DNA helix as the base-pairs are pushed apart to accommodate the bound ligand, leading to an increase in the DNA viscosity. In contrast, a partial, non-classical intercalation of ligand could bend (or kink) the DNA helix and reduce its effective length and, concomitantly, its viscosity. When outside binding occurs, the viscosity of DNA won't change basically [40,41].

Fig. 7 shows the effects of porphyrins **1–5** on the viscosity of rod-like DNA, which is very sensitive to the binding modes of the ligands. On increasing the amounts of **1** and **2**, the relative viscosity of DNA increases steadily. The increasing degree of viscosity, which may depend on its affinity to DNA, is **1**>**2**. However, the increasing of porphyrins **3**, **4**, **5** have no obvious effect on the relative viscosity of DNA. The viscosity results show that porphyrins **1** and **2** intercalate between the base-pairs of DNA, while the **3**, **4** and **5** bind to DNA in an outside binding mode. The distinct results of viscosity experiment convincingly prove the conclusion above.

3.2. Theoretical explanation to DNA-binding properties

According to the frontier molecular orbital theory, the higher occupied molecular orbital energy of one donor molecule and the lower unoccupied molecular orbital energy of the acceptor are advantageous to the interaction between the two molecules, because electrons more easily transferred from the occupied MOs of donor to the unoccupied MOs of acceptor [42]. A simple calculation model and calculated results by the DFT method for stacked DNA base-pairs with backbones have been reported by Kruita et al. [22]. The energies of the HOMO and HOMO−x (x=1–6) for the CG/CG stacking DNA calculated by the authors were −1.27, −1.33, −1.69, −1.79, −1.98, −2.06 and −2.08 eV, respectively. Fig. 8 displays some frontier molecular orbital energy levels of the title compounds calculated at the level of B3LYP/6-31G*. It is easy to find that the energies of the LUMO and LUMO+x (x=1–4) of these porphyrins are from −11.28 eV to −8.46 eV, which are much lower than those of the HOMO and HOMO−x (x=1–6) of the DNA base-pairs model. Therefore, the five porphyrins can interact with DNA strongly and should be good electron acceptors when binding to DNA. Moreover, we can see that the energies of LUMO and LUMO+x (x=1–4) of **1** are much lower than those of the tricationic porphyrins appending different phenyl substituents. Thus, it is easy to understand that K_b of **1** is much larger than those of the other four porphyrins based on the frontier molecular orbital theory.

On the other hand, the calculated results of Kurita show that the HOMO and HOMO−1 orbitals of DNA mostly populate on base-pairs and HOMO−x (x=2–4) mostly on phosphate functions [22]. From Fig. 9, LUMO and LUMO+1 for porphyrin **1**, LUMO and LUMO+x (x=1, 3) for porphyrin **2** have much component populated on the porphyrin core

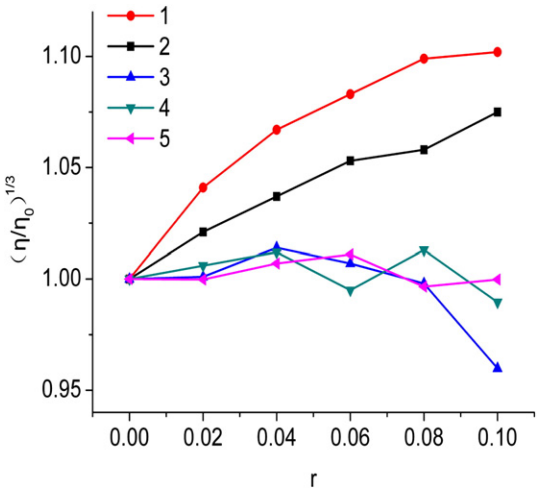

Fig. 7. Effects of increasing the amounts of porphyrins on the relative viscosities of CT DNA, in buffer A, at (30.0 ± 0. 1) °C; [DNA] = 0.5 mM. r = [Por]/[DNA].

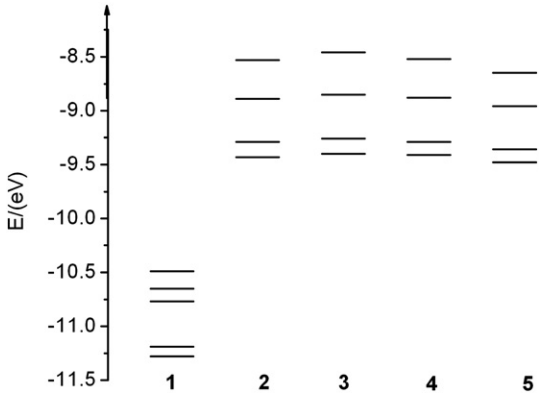

Fig. 8. Some frontier unoccupied orbital energies (in eV) of porphyrins **1–5** calculated at the level of B3LYP/6-31G*.

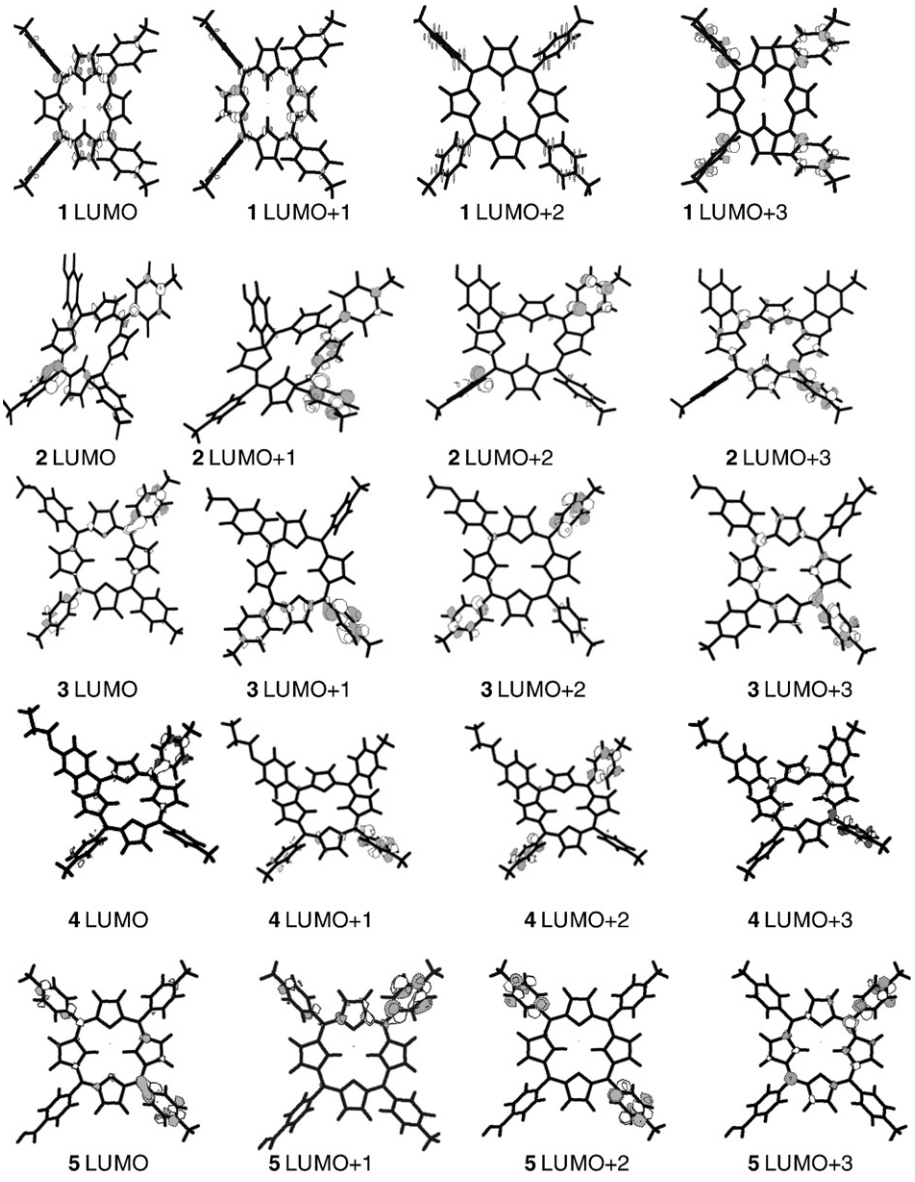

Fig. 9. Some frontier orbital contour of porphyrins **1**–**5** calculated at the level of B3LYP/6-31G*.

which is a big plane, while LUMO and LUMO+x (x=1–3) for the porphyrins **3**, **4**, **5** are mainly from the pyridine substituents. Thus, the interaction of porphyrins **1**, **2** and DNA may mainly through π–π stacking between porphyrin plane and base-pairs, in a classic intercalative mode. On the contrary, since there are high positive charges on the pyridine substituents, it is possible that the interaction of porphyrins **3**, **4**, **5** and DNA mainly through the electrostatic interaction between positively charged pyridines of the porphyrins and the negatively charged phosphate groups in the DNA backbone. Such explanation is in agreement with the experimental results.

At the same time, since the electrostatic strength is a strong driving force in the binding of cationic porphyrins to DNA [1–14], the natural charge population of porphyrin will be very important in determining its DNA-binding affinity. Higher natural population of positive charges on ligand is supposed to lead to a stronger interaction between the ligand and DNA. From Fig. 1, we can find that the only difference among the five porphyrins is the substituent group at *meso*-20 position of porphyrin core. The natural positive charges populated on the *meso*-20 substituent groups calculated at the level of B3LYP/6-31G* are given in Table 2, and follow an order of R1>>R3>R2>R4>R5. This order is

Table 2
The natural charge |e| of the substituent groups at *meso*-20-position of porphyrins **1**–**5**

1		2		3		4		5	
N1	−0.2961	C1	0.3640	C1	0.3659	C1	0.3434	C1	−0.1419
C2	−0.4770	O2	−0.6652	O2	−0.4995	O2	−0.5439	C2	0.8137
H3	0.2759	H3	0.5080	C3	−0.2573	C3	0.8442	O3	−0.5720
				H4	0.2277	O4	−0.5691	O4	−0.7043
						C5	−0.5669	H5	0.5180
R1	0.9404	R2	0.1528	R3	0.1760	R4	0.1345	R5	0.0833

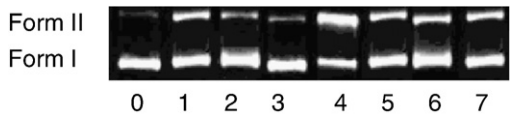

Fig. 10. Photocleavage of pBR322 DNA in the presence of porphyrin **2** and different inhibitors after irradiation by high pressure mercury lamp for 20 min, in buffer C. 10 μL reaction mixtures contained 1.0 μg of plasmid DNA. [Por]=1 μM. Lane 0: DNA control; lane 1: in the presence of porphyrin, no inhibitor; lanes 2–6: in the presence of porphyrin and inhibitor, (2) NaN_3 (5 mM), (3) under an Ar atmosphere, (4) 70%D_2O, (5) ethanol (5 mM), (6) methanol (5 mM), (7) DMSO (5 mM).

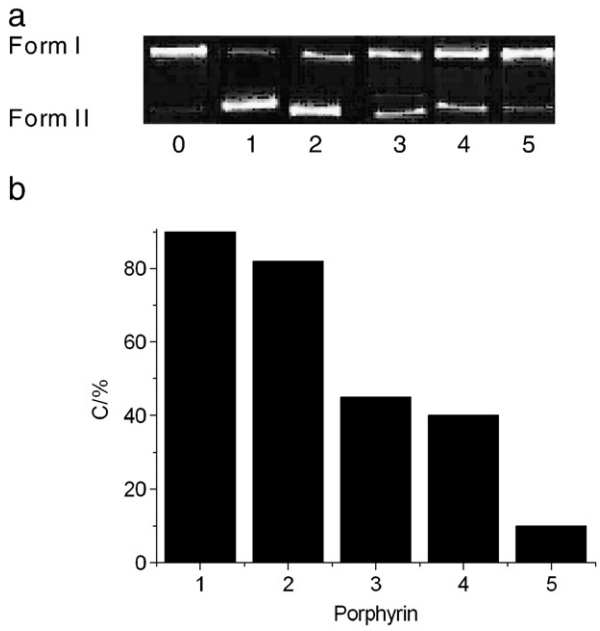

Fig. 11. (a): Photoactivated cleavage of pBR322 DNA in the presence of compounds, light after 20 min irradiation by high pressure mercury lamp, in buffer C. Lane 0: DNA controlled; Lanes 1 to 5: in the presence of 1 μm porphyrins **1**, **2**, **3**, **4** and **5**, respectively. (b): Percentage of Form II pBR322 DNA by irradiation of porphyrins.

similar to the porphyrins' K_b order except for porphyrins **2** and **3**, indicating that natural charge population is an important factor in determining the binding affinities. The exception can be easily understood by the larger steric hindrance of **3** than that of **2**. The larger steric hindrance may bring up obstacle for better binding mode and thus leads to a smaller binding constant, and this is consistent with the experimental results that the binding mode of porphyrin **2** is different from that of porphyrins **3**, **4**, **5**.

The above theoretical results can explain the DNA-binding properties of these porphyrins to a certain extent. However, our theoretical calculation skill is not so mature and needs further development. For example, modeling of the large DNA–porphyrin systems with molecular mechanics method instead of modeling isolated compounds with quantum chemistry method would provide valuable information for such kind of studies. Exploration on conquering this theoretical problem is in progress currently.

3.3. Photocleavage experiment

The cleavage reaction of porphyrins on plasmid DNA can be monitored by agarose gel electrophoresis. When circular plasmid DNA is subject to electrophoresis, relatively fast migration will be observed for the intact supercoil form (Form I). If scission occurs on one strand (nicking), the supercoil will relax to generate a slower-moving open circular form (Form II). If both strands are cleaved, a linear form (Form III) that migrates between Forms I and II will be generated [43].

Porphyrin has been reported to involve a $^1O_2$ mediated mechanism [18,44–46] in DNA cleavage. In order to establish the reactive species responsible for the DNA photocleavage by the studied five porphyrins, we investigated the influence of different potentially inhibiting agents. Porphyrin **2** was taken as an example and the result is shown in Fig. 10. Study with NaN_3, a $^1O_2$ quencher [20], was carried out and the cleavage was significantly inhibited (lane 2, Fig. 10). The photocleavage efficiency was also greatly inhibited when irradiation reaction was done under an Ar atmosphere (lane 3). On the other hand, the photocleavage ability was enhanced by replacing the reaction media H_2O by 70% D_2O which makes the life span of $^1O_2$ longer (lane 4). These results suggest that $^1O_2$ is likely to be one of the reactive species responsible for the cleavage reaction. Meanwhile, the cleavage of the plasmid DNA was not inhibited in the presence of hydroxyl radical ($OH^{\cdot}$) scavengers such as ethanol (lane 5), methanol (lane 6) and DMSO (lane 7) even at high concentration, suggesting that hydroxyl radical may not be the cleaving agent. Similar cases have also been observed for other four porphyrins under identical conditions (data not shown), indicating that $^1O_2$ is the reactive species responsible for the cleavage reaction of all these porphyrins.

Fig. 11a shows the DNA photocleavage results of the compounds under identical irradiation by high pressure lamp and Fig. 11b gives the percentage of Form II DNA formation. Without irradiation, no cleavage of DNA was observed for all the porphyrins (data not shown). Under comparative experimental conditions, the cleavage ability follows the order of **1**>**2**>**3**>**4**>**5**. It is found that the increasing order of DNA photocleavage activity of porphyrins is in parallel with the magnitude of their intrinsic binding constants (K_b) and the DNA intercalators (**1** and **2**) are more effective than the outside binders (**3**, **4** and **5**). The number of positive charges and the steric hindrance may be the key factors to influence their interactions with DNA. More positive charges and smaller steric hindrance of porphyrin will lead to a higher DNA photocleavage efficiency. These results are in high consistent with previous reports on the photocleavage of cationic porphyrins [47–50].

4. Conclusions

Based on absorption, fluorescence, CD spectra, thermal denaturation and viscosity measurements, the binding modes of four tricationic porphyrins to CT DNA were investigated in comparison with TMPyP. With a moderate ionic strength, the intrinsic DNA-binding constants of these tricationic porphyrins are much lower than that of TMPyP, suggesting that the number of positive charges is the main factor to affect the binding of cationic porphyrins to DNA. Among the four tricationic porphyrins, only porphyrin **2** with hydroxyphenyl group intercalates into DNA, while the other three porphyrins with larger steric hindrance bind to DNA in outside binding mode. This somewhat surprising result may be best understood by the steric hindrance effect. Theoretical calculations explain the above results via comparing the energy and population of the frontier orbitals, as well as the natural charge population of the porphyrins. Moreover, $^1O_2$ is proved to be the reactive species responsible for the cleavage reaction of all these porphyrins and a good correlation was observed between the DNA-binding affinity and photocleavage yield. These results are helpful in better understanding the DNA interactions of cationic porphyrins and may facilitate the design of new anticancer drugs.

Acknowledgements

We are grateful to the supports of Guangzhou Municipality Science and Technology Bureau of China, the National Natural Science Foundation of China and National Key Foundation Research Development Project (973) Item of China (No. 2007 CB815306).

References

[1] P. Hambright, E.B. Fleicher, The acid-base equilibria, kinetics of copper ion incorporation, and acid-catalyzed zinc ion displacement from the water-soluble porphyrin α, β, γ, δ-tetra(4-*N*-methylpyridyl)porphine, Inorg. Chem. 9 (1970) 1757–1761.
[2] R.J. Fiel, J.C. Howard, E.H. Mark, N.D. Gupta, Interaction of DNA with a porphyrin ligand: evidence for intercalation, Nucleic Acids Res. 6 (1979) 3093–3118.
[3] E.D. Mauro, R. Saladino, P. Tagliatesta, V.D. Sanctis, R. Negri, Manganese water-soluble porphyrin senses DNA conformation, J. Mol. Biol. 282 (1998) 43–57.
[4] W.K. Pogozelski, T.D. Tullius, Oxidative nucleobase modifications leading to strand scission, Chem. Rev. 98 (1998) 1089–1108.
[5] C.J. Burrows, J.G. Muller, Oxidative strand scission of nucleic acids: routes initiated by hydrogen abstraction from the sugar moiety, Chem. Rev. 98 (1998) 1109–1152.

[6] M. Sirish, H.J. Scheider, Porphyrin derivatives as water-soluble receptors for peptides, Chem. Commun. 10 (1999) 907–908.
[7] I. Haq, J.O. Trent, B.Z. Chowdhry, T.C. Jenkins, Intercalative G-tetraplex stabilization of telomeric DNA by a cationic Porphyrin, J. Am. Chem. Soc. 121 (1999) 1768–1779.
[8] L.H. Hurley, R.T. Wheelhouse, D. Sun, S.M. Kerwin, M. Salazar, O.Y. Fedoroff, F.X. Han, H. Han, E. Izbicka, D.D. Von Hoff, G-quadruplexes as targets for drug design, Pharmacol. Ther. 85 (2000) 141–158.
[9] R.F. Pasternack, E.J. Gibbs, A. Gaudemer, A. Antebi, S. Bassner, L.D. Poy, D.H. Turner, A. Williams, F. Laplace, M.H. Lansard, C. Merienne, M.P. Fauvet, Molecular complexes of nucleosides and nucleotides with a monomeric cationic porphyrin and some of its metal derivatives, J. Am. Chem. Soc. 107 (1985) 8179–8186.
[10] T. Uno, K. Hamasaki, M. Tanigawa, S. Shimabayashi, Binding of *meso*-tetrakis (*N*-methylpyridinium-4-yl)porphyrin to double helical RNA and DNA / RNA hybrids, Inorg. Chem. 36 (1997) 1676–1683.
[11] B. Armitage, Photocleavage of nucleic acids, Chem. Rev. 98 (1998) 1171–1200.
[12] A.B. Guliaev, N.B. Leontis, Cationic 5,10,15,20-tetrakis(*N*-methylpyridinium-4-yl) porphyrin fully intercalates at 5′-CG-3′ steps of duplex DNA in solution, Biochemistry 38 (1999) 15425–15437.
[13] T. Ohyama, H. Mita, Y. Yamamoto, Binding of 5,10,15,20-tetrakis(*N*-methylpyridinium-4-yl)-21*H*,23*H*-porphyrin to an AT-Rich Region of a Duplex DNA, Biophys. Chemist. 113 (2005) 53–59.
[14] R.F. Pasternack, E.J. Gibbs, J.J. Villafrancas, Interactions of porphyrins with nucleic acids, Biochemistry 22 (1983) 2406–2414.
[15] Y. Ishkava, A. Yamashita, T. Uno, Efficient photocleavage of DNA by cationic porphyrin–acridine hybrids with the effective length of diamino alkyl linkage, Chem. Pharm. Bull. 49 (3) (2001) 287–293.
[16] Y. Deng, C.K. Chang, D.G. Nocera, Facile synthesis of β-derivatized porphyrins—structural characterization of a β±β-bis-porphyrin, Angew. Chem., Int. Ed. 39 (2000) 1066–1068.
[17] J.O. Kim, Y.A. Lee, B. Jin, T. Park, R. Song, S.K. Kim, Binding mode of cationic monomer and dimer porphyrin with native and synthetic polynucleotides studied by polarized light spectroscopy, Biophys. Chem. 111 (2004) 63–71.
[18] S. Wu, Z. Li, L.G. Ren, B. Chen, F. Liang, X. Zhou, T. Jia, X.P. Cao, Dicationic pyridium porphyrins appending different peripheral substituents: synthesis and studies for their interactions with DNA, Bioorg. Med. Chem. 14 (2006) 2956–2965.
[19] H.D. Li, O.S. Fedorova, A.N. Grachev, W.R. Trumble, G.A. Bohach, L. Czuchajowski, A series of *meso*-tris *N*-methyl-pyridiniumyl-4-alkylamidophenyl porphyrins: synthesis, interaction with DNA and antibacterial activity, Biochim. Biophys. Acta 1354 (1997) 252–260.
[20] T. Jia, Z.X. Jiang, K. Wang, Z.Y. Li, Binding and photocleavage of cationic porphyrin–phenylpiperazine hybrids to DNA, Biophys. Chem. 119 (2006) 295–302.
[21] P. Zhao, L.C. Xu, J.W. Huang, K.C. Zheng, J. Liu, H.C. Yu, L.N. Ji, DNA binding and photocleavage properties of a novel cationic porphyrin–anthraquinone hybrid, Biophys. Chem. 134 (2008) 72–83.
[22] N. Kurita, K. Kobayashi, Density functional MO calculation for stacked DNA base-pairs with backbones, Comput. Chem. 24 (2000) 351–357.
[23] K.C. Zheng, J.P. Wang, W.L. Peng, X.W. Liu, F.C. Yun, Studies on 6,6′-disubstitution effects of the dpq in $[Ru(bpy)_2(dpq)]^{2+}$ with DFT method, J. Phys. Chem., A. 105 (2001) 10899–10905.
[24] W.J. Mei, J. Liu, K.C. Zheng, L.J. Lin, H. Chao, A.X. Li, F.C. Yun, L.N. Ji, Experimental and theoretical study on DNA-binding and photocleavage properties of chiral complexes Δ- and Λ-$[Ru(bpy)_2L]$(L=*o*-hpip, *m*-hpip and *p*-hpip), Dalton Trans. 7 (2003) 1352–1359.
[25] K.C. Zheng, X.W. Liu, J.P. Wang, F.C. Yun, L.N. Ji, DFT studies on the molecular orbitals and related properties of $[Ru(phen)_2(9,9'\text{-}2R\text{-}dpq)]^{2+}$(R=$NH_2$,OH,H and F), J. Mol. Struct. (Theochem) 637 (2003) 195–203.
[26] H. Xu, K.C. Zheng, H. Deng, L.J. Lin, Q.L. Zhang, L.N. Ji, Effects of the ancillary ligands of polypyridyl ruthenium(II) complexes on the DNA-binding behaviors, New J. Chem. 27 (2003) 1255–1263.
[27] A.D. Adler, F.R. Longo, J.D. Finarelli, J. Goldmacher, K.J. Assour, A simplified synthesis for *meso*-tetraphenylporphine, J. Org. Chem. 32 (1967) 476–477.
[28] M.E. Reichmann, S.A. Rice, C.A. Thomas, P. Doty, A further examination of the molecular weight and size of desoxypentose nucleic acid. J. Am. Chem. Soc. 76 (1954) 3047–3053.
[29] M.J. Frisch, G.W. Trucks, H.B. Schlegel, G.E. Scuseria, M.A. Robb, J.R. Cheeseman, J.A. Montgomery Jr., T. Vreven, K.N. Kudin, J.C. Burant, J.M. Millam, S.S. Iyengar, J. Tomasi, V. Barone, B. Mennucci, M. Cossi, G. Scalmani, N. Rega, G.A. Petersson, H. Nakatsuji, M. Hada, M. Ehara, K. Toyota, R. Fukuda, J. Hasegawa, M. Ishida, T. Nakajima, Y. Honda, O. Kitao, H. Nakai, M. Klene, X. Li, J.E. Knox, H.P. Hratchian, J.B. Cross, V. Bakken, C. Adamo, J. Jaramillo, R. Gomperts, R.E. Stratmann, O. Yazyev, A.J. Austin, R. Cammi, C. Pomelli, J.W. Ochterski, P.Y. Ayala, K. Morokuma, G.A. Voth, P. Salvador, J.J. Dannenberg, V.G. Zakrzewski, S. Dapprich, A.D. Daniels, M.C. Strain, O. Farkas, D.K. Malick, A.D. Rabuck, K. Raghavachari, J.B. Foresman, J.V. Ortiz, Q. Cui, A.G. Baboul, S. Clifford, J. Cioslowski, B.B. Stefanov, G. Liu, A. Liashenko, P. Piskorz, I. Komaromi, R.L. Martin, D.J. Fox, T. Keith, M.A. Al-Laham, C.Y. Peng, A. Nanayakkara, M. Challacombe, P.M.W. Gill, B. Johnson, W. Chen, M.W. Wong, C. Gonzalez, J.A. Pople, Gaussian 03, Revision D.01, Gaussian, Inc., Wallingford CT, 2005.
[30] T. Masaaki, K.S. Ashish, N. Elvis, Enhanced conformational changes in DNA in the presence of mercury(II), cadmium(II) and lead(II) porphyrins, J. Inorg. Biochem. 94 (2003) 50–58.
[31] M.A. Sari, J.P. Battioni, D. Dupre, D. Mansuy, J.B. Lepecq, Interaction of cationic porphyrins with DNA: importance of the number and position of the charges and minimum structural requirements for intercalation, Biochemistry 29 (1990) 4205–4215.
[32] N.E. Mukundan, G. Petho, D.W. Dixon, M.S. Kim, L.G. Marzilli, Interactions of an electron-rich tetracationic tentacle porphyrin with calf thymus DNA, Inorg. Chem. 33 (1994) 4676–4687.
[33] E. Nyarko, N. Hanada, A. Habib, M. Tabata, Fluorescence and phosphorescence spectra of Au(III), Pt(II) and Pd(II) porphyrins with DNA at room temperature, Inorg. Chim. Acta 357 (2004) 739–745.
[34] T. Masaaki, K.S. Ashish, N. Elvis, Enhanced conformational changes in DNA in the presence of mercury(II), cadmium(II) and lead(II) porphyrins, J. Inorg. Biochem. 94 (2003) 50–58.
[35] J.M. Kelly, A.B. Tossi, D.J. McConell, C. OhUigin, A study of the interactions of some polypyridylruthenium(II) complexes with DNA using fluorescence spectroscopy, topoisomerisation and thermal denaturation, Nucl. Acids Res. 13 (1985) 6017–6034.
[36] T. Uno, K. Hamasaki, M. Tanigawa, S. Shinabayashi, Binding of *meso*-tetrakis (*N*-methylpyridinium-4-yl)porphyrin to double helical RNA and DNA•RNA hybrids, Inorg. Chem. 36 (1997) 1676–1683.
[37] R. Kuroda, H. Tanaka. DNA–porphyrin interactions probed by induced CD spectroscopy, J. Chem. Soc., Chem. Commun. 13 (1994) 1575–1576.
[38] E. Nyarko, M. Tabata, Interactions of tetracationic mercury(II), cadmium(II) and lead(II) porphyrins with DNA and their effects on DNA cleavage, J. Porphyr. Phthalocyanines 5 (2001) 873–880.
[39] H.T. Daryono, M. Shunsuke, A. Takehiro, Y. Naoki, I. Hidenari, Interaction of metallopyrazoliumylporphyrins with calf thymus DNA, J. Inorg. Biochem. 85 (2001) 219–228.
[40] S. Satyanarayana, J.C. Dabrowiak, J.B. Chaires, Tris(phenanthroline)ruthenium(II) enantiomer interactions with DNA: mode and specificity of binding, Biochemistry 32 (1993) 2573–2584.
[41] V.A. Bloomfield, D.M. Crothers, I. Tinoko Jr. (Eds.), Nucleic Acids: Structures, Properties, and Functions, University Science Books, California, 2000, pp. 535–596, Chapter 11.
[42] I. Fleming, Frontier Orbital and Organic Chemical Reaction, Wiley, New York, 1976.
[43] J.K. Barton, A.L. Raphael, Photoactivated stereospecific cleavage of double-helical DNA by cobalt(III) complexes, J. Am. Chem. Soc. 106 (1984) 2466–2468.
[44] T.J. Dougherty, C.J. Gomer, B.W. Henderson, G. Jori, D. Kessel, M. Korbelik, J. Moan, Q. Peng, Photodynamic therapy, J Natl Cancer Inst. 90 (1998) 889–905.
[45] E.D. Sternberg, D. Dolphin, C. Bruckner, Porphyrin-based photosensitizers for use in photodynamic therapy, Tetrahedron 54 (1998) 4151–4202.
[46] R. Bonnett, Chemical Aspects of Photodynamic Therapy, Gordon and Breach Science, Amsterdam, 2000.
[47] S. Mettath, B.R. Munson, R.K. Pandey, DNA interaction and photocleavage properties of porphyrins containing cationic substituents at the peripheral position, Bioconjug. Chem. 10 (1999) 94–102.
[48] Bruce Armitage, Photocleavage of nucleic acids, Chem. Rev. 98 (1998) 1171–1200.
[49] S.R. Chatterjee, T.S. Srivastava, J.P. Kamat, T.P.A. Devasagayam, Photocleavage of plasmid pBR322 DNA by some anionic porphyrins, J. Porphyr. Phthalocyanines 2 (1998) 337–343.
[50] H. Taima, A. Okubo, N. Yoshioka, H. Inoue, DNA-binding properties and photocleavage activity of cationic water-soluble chlorophyll derivatives, Chem. Eur. J. 12 (2006) 6331–6340.